CHIN. PHYS. LETT. Vol. 38, No. 5 (2021) 058201

Electrochemical Behavior of Vanadium Carbide in Neutral Aqueous Electrolytes

Chaofan Chen(陈超凡)[1], Di Pang(庞迪)[1], Xiaotong Wang(王晓彤)[1], Gang Chen(陈岗)[1,2], Fei Du(杜菲)[1,2*], and Yu Gao(高宇)[1*]

[1]*Key Laboratory of Physics and Technology for Advanced Batteries (Ministry of Education), College of Physics, Jilin University, Changchun 130012, China*

[2]*State Key Laboratory of Superhard Materials, College of Physics, Jilin University, Changchun 130012, China*

(Received 10 January 2021; accepted 5 March 2021; published online 2 May 2021)

The V_2C compound, belonging to the group of two-dimensional transition metal carbonitrides, or MXenes, has demonstrated a promising electrochemical performance in capacitor applications in acidic electrolytes; however, there is evidence to suggest that V_2C is unstable in an acidic environment. On the other hand, the performance of V_2C in neutral aqueous electrolytes is still moderate, and has not yet been systematically studied. The charge storage mechanism in a V_2C electrode, employed in neutral aqueous electrolytes, is investigated via cyclic voltammetry testing and *in situ* x-ray diffraction (XRD). Good specific capacitances are achieved, specifically 208 F/g in 0.5 M Li_2SO_4, 225 F/g in 1 M $MgSO_4$, 120 F/g in 1M Na_2SO_4, and 104 F/g in 0.5 M K_2SO_4. Using *in situ* XRD, we observe that, during the charge and discharge process, the *c*-lattice parameter shrinks or expands by up to 0.25 Å in $MgSO_4$, and 0.29 Å in Li_2SO_4 which demonstrates the intercalation/de-intercalation of cations into the *d*-V_2C layer.

DOI: 10.1088/0256-307X/38/5/058201

MXene, a family of two-dimensional transition metal carbides/nitrides, synthesized by selectively removing the A element from the precursor phase, $M_{n+1}AX_n$ (where M is an early transition metal, A stands for any element from the ⅢA and ⅣA groups, X is C and/or N, and $n = 1$, 2, or 3), has attracted much attention due to their versatile composition, high conductivity and hydrophilic surface.[1,2] There are currently more than thirty known MXene materials, including Ti_3C_2,[3] Ti_2C,[4] Nb_4C_3,[5] Nb_2C,[6] and V_2C.[7] The particular relevance of this kind of material is its potential application in the field of energy storage;[8−11] as such, the charge storage mechanisms of MXenes in different electrolytes have been studied.[12−16] The majority of studies have focused on Ti_3C_2, the most widely investigated member of the MXene group, and a possible mechanism for its intercalation/de-intercalation has been proposed.[3]

V_2C, one of the lightest MXene materials, possessing a unique vanadium metal layer, tends to achieve high specific capacity due to its variable valence (V^{2+}, V^{3+}, V^{4+}, V^{5+}) during electrochemical processes. Vanadium carbide was first synthesized in 2013, when it was used as the negative electrode for a lithium ion battery; a capacity of 260 mAh/g was achieved at 1 C, and a high rate performance was reported.[17] Since then, many studies have been devoted to the energy storage applications of V_2C materials. Dall'Agnese *et al.*[7] investigated V_2C as a positive electrode in a sodium ion capacitor, and achieved a specific capacitance of 100 F/g at a scan rate of 0.2 mV/s. Bak *et al.* studied a V_2C anode material for Na-ion batteries, reporting on the redox reaction of vanadium as a charge-storage mechanism.[18] Wang *et al.* examined V_2C intercalated with cobalt ions, demonstrating its capacity to realize an ultra-long cycle life of more than 15000 cycles, and a high specific Lithium storage capacity of 686.7 mAh/g at 0.1 C, due to the enlarged interlayer space, and the formation of a V–O–Co bond.[19] In addition, CNT@V_2C was investigated by the same team, in the context of a Zn-ion supercapacitor with 190.2 F/g at 0.5 A/g.[20] The use of few-layer V_2C was also investigated in an aluminum ion battery, where the reversible intercalation/de-intercalation of aluminum cations was suggested as the mechanism for charge storage.[21]

In our previous work, V_2C was investigated as an electrode material in an aqueous electrolyte (H_2SO_4, KOH, and $MgSO_4$) for supercapacitors, and impressive capacitance was demonstrated.[22] In this work, we investigate the electrochemical behavior of V_2C in different neutral aqueous electrolytes (Li_2SO_4, Na_2SO_4, K_2SO_4, and $MgSO_4$), and further explore its reaction mechanisms via *in situ* XRD, taking into account that neutral electrolytes are more environmentally friendly, cheaper and safer, that the *d*-V_2C ma-

Supported by the Science & Technology Department of Jilin Province (Grant Nos. 20180101199JC and 20180101204JC), and Jilin Province/Jilin University Co-construction Project-Funds for New Materials (SXGJSF2017-3).

*Corresponding authors. Email: yugao@jlu.edu.cn; dufei@jlu.edu.cn

© 2021 Chinese Physical Society and IOP Publishing Ltd

terial is unstable in acidic electrolytes, and that the dissolution of vanadium may occur during cycling.[22]

Experiment. Firstly, 1 g V_2AlC powder (200 mesh, purchased from Jilin 11 technology Co.) was slowly added into 20 ml HF (49% HF, Aladdin) and stirred for five days at 25℃. The resulting dark green solution was dispersed in DI water, and centrifuged several times at 5000 rpm to obtain a final precipitation at pH ∼ 6. The precipitation was then dried at 60℃ in a vacuum oven to produce V_2C powder. Next, 0.3 g of V_2C, suspended in 18 mL of deionized H_2O, was mixed with 2 ml TMAOH (25% TMAOH in water, Aladdin), and stirred for 15 h at room temperature. Residual TMAOH was removed by means of repeated centrifugation at 5000 rpm. The stable delaminated V_2C colloidal solutions (d-V_2C) were collected after 30 min of sonication and 1 h of centrifugation at 3500 rpm, and a free-standing d-V_2C film was then acquired via vacuum-assisted filtration.

Scanning electron microscopy (SEM, JSM-6700 F) was employed to observe the morphology of the resulting V_2C. X-ray diffraction patterns were collected using a Bruker D8 diffractometer, operated at 40 kV and 40 mA, with Cu K_α radiation ($\lambda = 1.5406$ Å).

A flexible, binder-free d-V_2C film was used directly as the working electrode, with a counter-electrode comprising over-capacitive activated carbon, containing 5 wt% PTFE, and a reference electrode composed of Ag wire. Here, 0.5 M Li_2SO_4, 0.5 M Na_2SO_4, 0.5 M K_2SO_4, and 1 M $MgSO_4$ solutions were used as electrolytes, with cellulose membrane functioning as the separator. Three-electrode Swagelok cells were assembled and tested using a VMP3 potentiostat (Biologic, S.A.). Electrochemical impedance spectroscopy (EIS) measurements were carried out at open circuit potential, with an amplitude of 10 mV, in a frequency range between 100 kHz and 10 mHz. For the *in situ* XRD test, plastic modified three-electrode cells were assembled with same selection of electrodes as those used in the electrochemical tests above. Cyclic Voltammetry was performed at 0.5 mV/s to control the working electrode potential, using a Vertex-One device, provided by Ivium Technologies B.V. The *in situ* XRD patterns were recorded in the range of $2\theta = 5$–$10°$ with steps of 0.02°.

Results and Discussion. Figure 1(a) illustrates the XRD patterns of V_2AlC, before and after HF etching, and of the d-V_2C film obtained via vacuum filtration. Due to the uneven etching process, the XRD pattern of the etched particles showed two new peaks (at 9.2° and 10.9°), corresponding to the (002) plane of V_2C MXene, while unreacted V_2AlC remained dominant. During the delamination process, we found a significant decrease in the (002) peak between V_2C and the d-V_2C film, corresponding to the c-lattice parameter from 16.2 Å and 19.2 Å to 24.3 Å, indicating the intercalation of TMA^+.[23]

An SEM image of the V_2C sample is shown in Fig. 1(b). The sample exhibits the typical accordion-like structure of MXene, and the cross-section scanning electron microscope image of the d-V_2C film in Fig. 1(c) shows that the film is composed of re-stacked nanosheets.

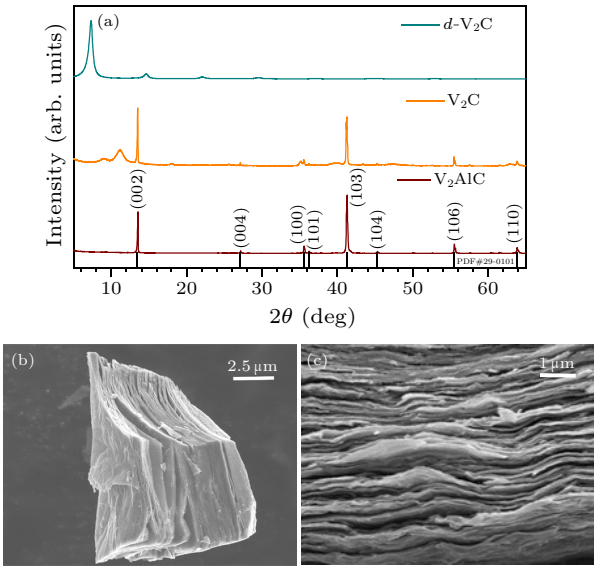

Fig. 1. (a) XRD patterns of V_2AlC, V_2C, and d-V_2C film after delamination. (b) SEM image of V_2C after etching. (c) SEM image of filtrated d-V_2C paper.

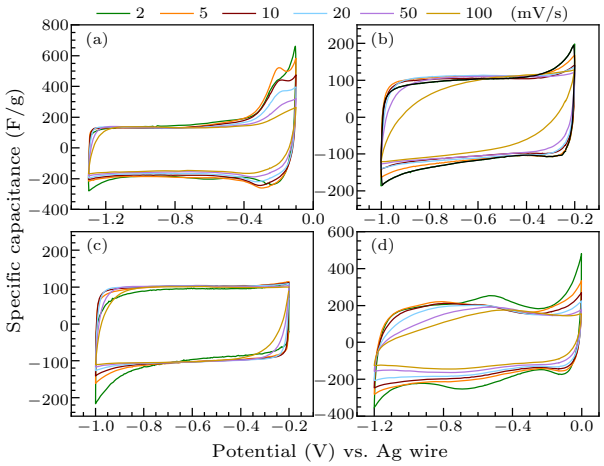

Fig. 2. Cyclic voltammograms of d-V_2C at different scan rates in (a) 0.5 M Li_2SO_4, (b) 0.5 M Na_2SO_4, (c) 0.5 M K_2SO_4, and (d) 1 M $MgSO_4$.

The electrochemical behavior of the d-V_2C film was investigated in various neutral electrolytes: 0.5 M Li_2SO_4, 0.5 M Na_2SO_4, 0.5 M K_2SO_4, and 1 M $MgSO_4$. Figure 2 shows the cyclic voltammograms. The C–V curves obtained in the 0.5 M Na_2SO_4 and 0.5 M K_2SO_4 electrolytes were nearly ideal—rectangular, and without any visible redox peaks, suggesting the typical EDLC charge storage mechanism.[24,25] However, since the double-layer ca-

pacitance is proportional to the specific surface area of electrode, much lower capacitance would be expected with the low SSA of the MXene material if EDLC were the only charge storage mechanism.[3] It is therefore more likely that Na^+ and K^+ could access some shallow sites in the d-V_2C film, thereby contributing to the total capacitance. In addition, the shape of the C–V curves remained rectangular, and without obvious distortion, with increasing scan rate, which demonstrates an impressive rate performance. With respect to the 0.5 M Li_2SO_4 electrolyte, the cyclic voltammogram exhibited an overall rectangular shape, with an obvious peak at around −0.2 V versus. Ag, and a reduction peak which was broad and less pronounced. Upon cycling in 1 M $MgSO_4$ at 2 mV/s, a pair of broad reduction peaks were evident at around −0.7 V versus Ag, which implies the possible electrochemical intercalation of cations.[3]

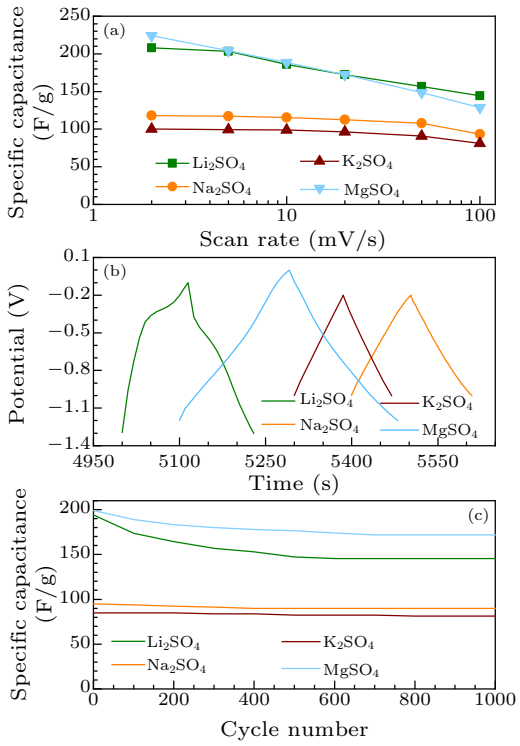

Fig. 3. Electrochemical performance of d-V_2C electrode. (a) Specific capacitance measured from corresponding C–V patterns. (b) Galvanostatic charge and discharge profiles at 1 A/g for different electrolytes. (c) Cycle lives measured from galvanostatic charge to discharge at 1 A/g.

Figure 3(a) summarizes the specific capacitance obtained at different scan rates. A high specific capacitance of 225 F/g was obtained at 2 mV/s in 1 M $MgSO_4$; when the scan rate was increased to 100 mV/s, the capacitance decreased to a moderate value of 130 F/g. In 0.5 M Li_2SO_4, a better rate performance was demonstrated, with capacitance of 208 F/g and 160 F/g at 2 mV/s and 100 mV/s, respectively. The higher capacitance in Li_2SO_4 and $MgSO_4$ may be attributed to charge transfer between the intercalated cations and MXene, in addition to surface adsorption capacitance; charge redistribution occurs via orbital coupling between the surface termination and ions, leading to depletion of the electrostatic potential difference.

Figure 3(b) shows the GCD curves of the d-V_2C electrode at a current density of 1 A/g. There was a plateau at around −0.3 V in 0.5 M Li_2SO_4, consistent with the C–V test. In addition, linear GCD curves were obtained in 0.5 M Na_2SO_4 and 0.5 M K_2SO_4 without an obvious IR drop. The cycle life of the d-V_2C, tested by galvanostatic charge-discharge at a high current density of 1 A/g, is given in Fig. 3(c). The capacitance values obtained in 0.5 M Na_2SO_4 and 0.5 M K_2SO_4 were 96 F/g and 83 F/g, respectively, and remained stable at around 97% and 98% after 1000 cycles. The capacitance slightly decreased with the number of cycles in Li_2SO_4 and $MgSO_4$, and capacitance retention levels after 1000 cycles were 75% and 87.5%, respectively. To explore the electrochemical kinetic of different ions, the pseudocapacitive contribution of MXene in $MgSO_4$ and Li_2SO_4 is illustrated in Fig. S1 in the Supplemental Material; the capacitive contribution is increased, with a maximum value of 92.1% in Li_2SO_4, and 87.3% in $MgSO_4$ at 100 mV/s with an increase in the scan rate. Moreover, the capacitive contribution was found to be 69.7% at 10 mV/s in Li_2SO_4, higher than the 59.3% found in $MgSO_4$, consistent with its reasonable rate performance. Electrochemical impedance spectroscopy (EIS) was also performed to investigate the internal resistance and ion-diffusion process. As shown in Fig. S2, there is no visible semicircle in any electrolyte, which corresponds to low charge transfer resistance (R_{ct}). In 0.5 M K_2SO_4, the equivalent high-frequency resistance (ESR) determined by the intersection of the high-frequency arc and the real axis is lower than for the other electrolytes, indicating that the inherent resistance in the cell is lower.

Figure S3 shows the XRD patterns of a d-V_2C electrode immersed in 0.5 M Li_2SO_4 and 1 M $MgSO_4$ electrolytes. When immersed in the electrolytes, shift of peaks occurred, which may be attributed to the spontaneous intercalation of cations.[26] The *in situ* x-ray diffraction was used to further verify the intercalation of Li^+ and Mg^{2+} during cycling. Figures 4(a) and 4(b) are contour maps of the *in situ* XRD patterns collected in the range $2\theta = 5°$–$10°$ during cyclic voltammetry in Li_2SO_4 and $MgSO_4$. A clear shift of (002) was visible during cycling in both electrolytes, confirming the intercalation/de-intercalation phenomenon of Li^+ and Mg^{2+} into d-V_2C. Figures 4(c) and 4(d) show the change in the c-lattice parameter, depending on the potential during the first three cycles. A slight shrink-

age of the c value was observed with increasing voltage, which could be attributable to the electrostatic attraction interaction between positively charged solvated cations and the negatively charged MXene surface. For example, the first cycle in Li_2SO_4 showed that the c-lattice parameter decreased continuously to 24.61 Å from 24.32 Å, from −0.1 to −1.3 V, versus Ag, then expanded continuously to 24.58 Å when the potential returned to −0.1 V. The c-lattice parameter therefore changed by as much as 0.29 Å during this single cycle; the irreversible change in the c value after each cycle could be explained by incomplete extraction of Li^+, and shrinkage of the interlayer space may lead to the observed decrease in capacitance. The c-lattice parameter changed by up to 0.25 Å in $MgSO_4$ during a single cycle, and was reversible during cycling.

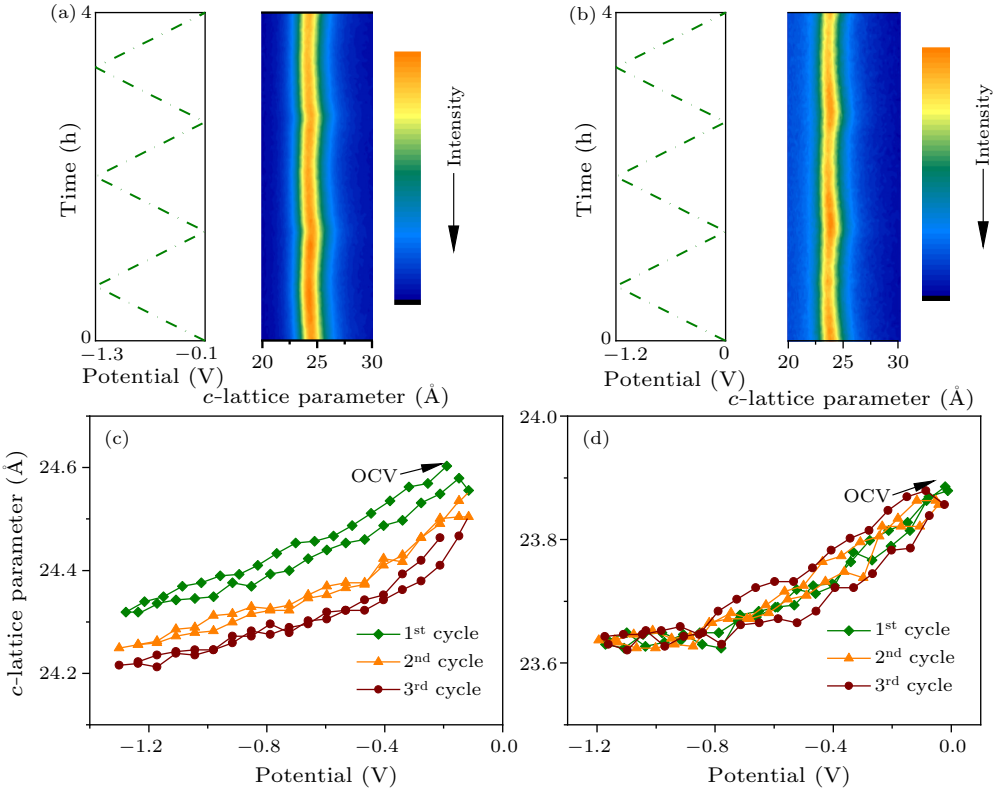

Fig. 4. *In situ* XRD patterns of *d*-V_2C during electrochemical cycles in (a) 0.5 M Li_2SO_4, and (b) 1 M $MgSO_4$. Change of the c-lattice parameter with potential during the first 3 cycles in (c) 0.5 M Li_2SO_4, and (d) 1 M $MgSO_4$.

In general, the multi-scale computation method is a useful tool helpful to reveal the electrochemical storage principle of an energy-storage material,[27] MXene is no exception. Mu *et al.* combined DFT calculations and an *in situ* XRD technique to investigate the charge-storage mechanism of MXene in H_2SO_4, and confirmed that the c-lattice of Ti_3C_2 can change with H^+ intercalation, due to the steric effect, together with electrostatic force.[15] By combining first-principles calculations and the implicit solvation model and investigating the electronic states during charge process, Ando *et al.* proposed the interaction between partially intercalated dehydrated cations and MXene layers.[28] We can deduce that the charge-storage mechanism of V_2C may be closely related to the size of cations; cations with smaller ion radii, such as Mg^{2+} and Li^+, could intercalate into the interlayer space, and interact with the surface V atom and termination groups, as illustrated in Fig. 5, while larger ions such as Na^+ and K^+ could only access a few shallow sites, thereby contributing to superior rate and cycling performance.

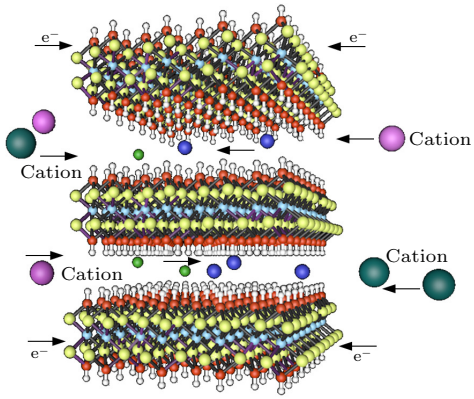

Fig. 5. Schematic illustration of V_2C during the discharge process. (yellow, V; sky blue, C; red, O; white, H; interlayer species: cations with different ion radius).

In summary, we have investigated the charge storage mechanism in V_2C electrode in various neutral

aqueous electrolyte via cyclic voltammetry and *in situ* XRD, and good electrochemical performance is achieved. Redox peaks are visible in the C–V patterns in $MgSO_4$ and Li_2SO_4, and a slight shrinkage in the c value of 0.25 Å in $MgSO_4$, and 0.29 Å in Li_2SO_4 is observed with increasing voltage by means of *in situ* XRD. This definitively demonstrates the presence of cation intercalation into the d-V_2C layer. The superior cycle life of $MgSO_4$ can also be explained by the reversible change in the c value during cycling, while the lower capacitance retention of Li_2SO_4 is attributed to the shrinkage of interlayer space during cycling. In Na_2SO_4 and K_2SO_4, nearly rectangular C–V patterns with great cycling performance are demonstrated, in spite of their modest capacitance. In conclusion, the practical application of V_2C materials in aqueous electrolytes can be realized in a neutral environment, and careful selection of electrolytes with different cations should be considered for different demands: larger cations are suitable for energy storage devices where a long cycle life is a major requirement, while smaller cations are able to fulfill a requirement for high capacitance.

The authors particularly wish to express their appreciation to Professor Yohan Dall'Agnese for great advice and support to this paper.

References

[1] Naguib M et al 2012 *ACS Nano* **6** 1322
[2] Naguib M et al 2014 *Adv. Mater.* **26** 992
[3] Lukatskaya M R et al 2013 *Science* **341** 1502
[4] Come J et al 2012 *J. Electrochem. Soc.* **159** A1368
[5] Zhao S S et al 2017 *Energy Storage Mater.* **8** 42
[6] Mashtalir O et al 2015 *Adv. Mater.* **27** 3501
[7] Dall'Agnese Y et al 2015 *J. Phys. Chem. Lett.* **6** 2305
[8] Naguib M et al 2012 *Electrochem. Commun.* **16** 61
[9] Ghidiu M et al 2014 *Nature* **516** 78
[10] Wang X et al 2015 *Nat. Commun.* **6** 6544
[11] Lukatskaya M R et al 2017 *Nat. Energy* **2** 17105
[12] Levi M D et al 2015 *Adv. Energy Mater.* **5** 1400815
[13] Lukatskaya M R et al 2015 *Adv. Energy Mater.* **5** 1500589
[14] Lin Z F et al 2016 *Electrochem. Commun.* **72** 50
[15] Mu X P et al 2019 *Adv. Funct. Mater.* **29** 1902953
[16] Wang X H et al 2019 *Nat. Energy* **4** 241
[17] Naguib M et al 2013 *J. Am. Chem. Soc.* **135** 15966
[18] Bak S M et al 2017 *Adv. Energy Mater.* **7** 1700959
[19] Wang C D et al 2018 *Adv. Mater.* **30** 1802525
[20] Wang C D et al 2019 *Small Methods* **3** 1900495
[21] VahidMohammadi A et al 2017 *ACS Nano* **11** 11135
[22] Shan Q M et al 2018 *Electrochem. Commun.* **96** 103
[23] Mashtalir O et al 2013 *Nat. Commun.* **4** 1716
[24] Simon P and Gogotsi Y 2008 *Nat. Mater.* **7** 845
[25] Wang G P et al 2012 *Chem. Soc. Rev.* **41** 797
[26] Ghidiu M et al 2016 *Chem. Mater.* **28** 3507
[27] Shi S Q et al 2016 *Chin. Phys. B* **25** 018212
[28] Ando Y et al 2020 *Adv. Funct. Mater.* **30** 2000820

Supplemental Material for "Electrochemical Behavior of Vanadium Carbide in Neutral Aqueous Electrolytes"

Chaofan Chen(陈超凡)[1], Di Pang(庞迪)[1], Xiaotong Wang(王晓彤)[1], Gang Chen(陈岗)[1,2], Fei Du(杜菲)[1,2*], Yu Gao(高宇)[1*]

[1]Key Laboratory of Physics and Technology for Advanced Batteries

(Ministry of Education), College of Physics, Jilin University, Changchun 130012, Jilin, P R China

[2]State Key Laboratory of Superhard Materials, College of Physics,

Jilin University, Changchun 130012, Jilin, P R China

Contact information:

corresponding author: yugao@jlu.edu.cn, 17790011805

dufei@jlu.edu.cn, 13514491857

First author: cfchen98@163.com, 18443154660

Second author: pangdi19@mails.jlu.edu.cn,16688209392

For systems exhibiting capacitive and semi-infinite linear diffusion process, the current (i) for capacitive process of a cyclic voltammetry experiment is proportional to sweep rate(υ), while the current of diffusion limited process is proportional to $\upsilon^{1/2}$. the current flowing at a specific potential i(V) is defined as:

$$i(V)=k_1\upsilon+k_2\upsilon^{1/2} \quad \ldots\ldots (1)$$

where k_1 and k_2 are fitting parameters. A plot of $i(V)/\upsilon^{1/2}$ versus $\upsilon^{1/2}$ should produce a straight line from which k_1 and k_2 can be determined, and hence the contributions to capacitive and diffusive current can be deduced[1].

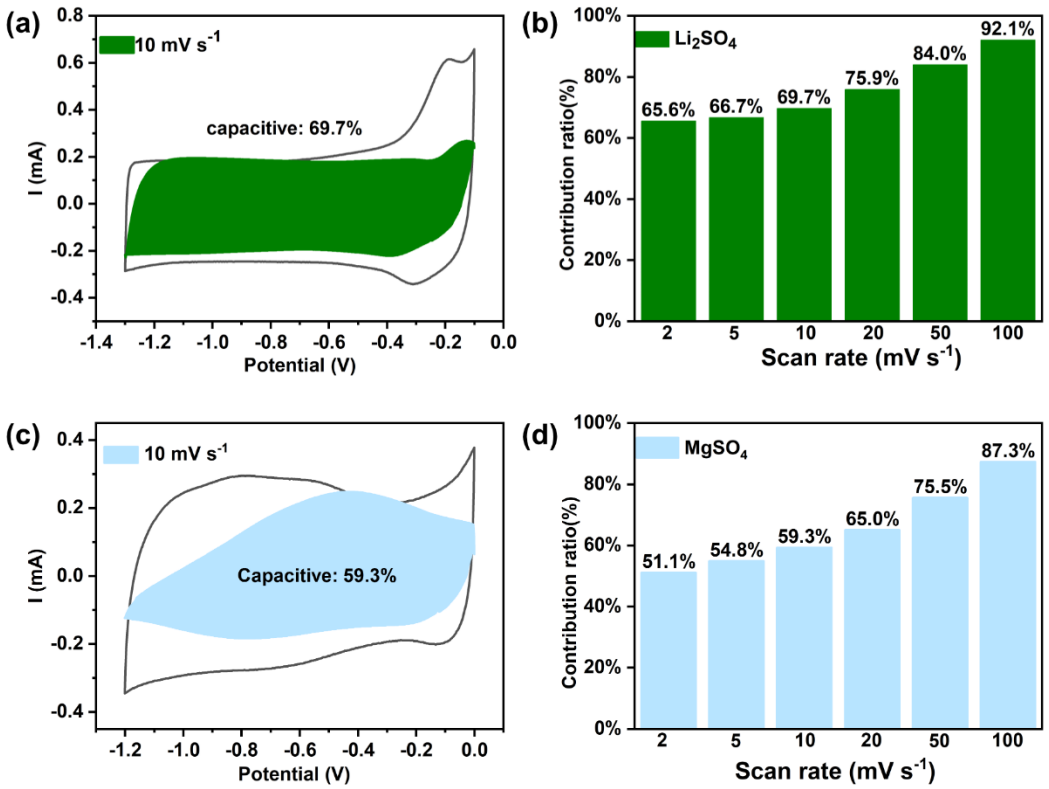

Figure.S1 capacitive contribution of d-V_2C in Li_2SO_4 (a), (b) and $MgSO_4$ (c), (d)

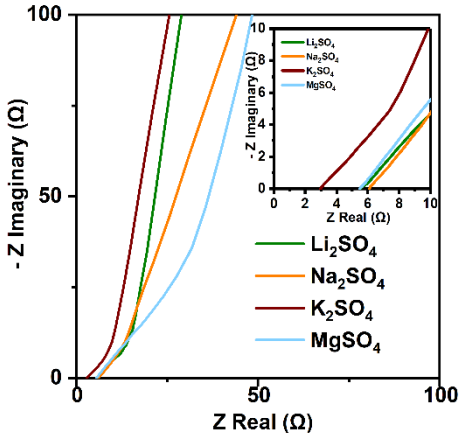

Figure.S2 Nyquist plot from EIS.

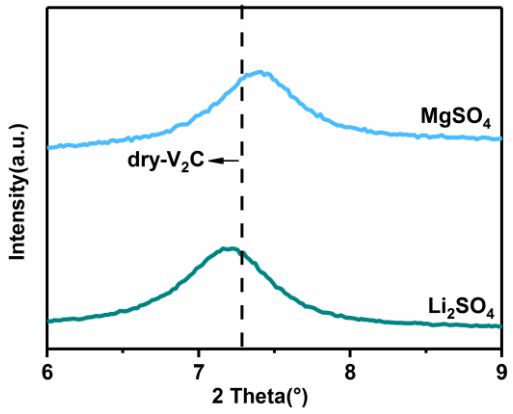

Figure.S3 XRD patterns of d-V_2C dry and immersed in 0.5 M Li_2SO_4 and 1 M $MgSO_4$. Electrochemical in situ X-Ray diffraction study of d-V_2C in different electrolytes.

Reference

[1]Augustyn V, Come J, Lowe M A, Kim J W, Taberna P-L, Tolbert S H, Abruña H D, Simon P and Dunn B 2013 *Nature Materials* **12** 518